CRITICAL CURRENT DENSITY AND MICROSTRUCTURE VARIATIONS IN YBa$_2$Cu$_3$O$_{7-x}$ + BaSnO$_3$ FILMS WITH DIFFERENT CONCENTRATIONS OF BaSnO$_3$ (POSTPRINT)

C.V. Varanasi, J. Burke, and L. Brunke

University of Dayton Research Institute

H. Wang and J.H. Lee

Texas A&M University

P.N. Barnes

Mechanical Energy Conversion Branch
Energy/Power/Thermal Division

FEBRUARY 2012

STINFO COPY

AIR FORCE RESEARCH LABORATORY
PROPULSION DIRECTORATE
WRIGHT-PATTERSON AIR FORCE BASE, OH 45433-7251
AIR FORCE MATERIEL COMMAND
UNITED STATES AIR FORCE

REPORT DOCUMENTATION PAGE

Form Approved
OMB No. 0704-0188

1. REPORT DATE *(DD-MM-YY)*	2. REPORT TYPE	3. DATES COVERED *(From - To)*
February 2012	Journal Article Postprint	19 June 2006 – 19 June 2008

4. TITLE AND SUBTITLE

CRITICAL CURRENT DENSITY AND MICROSTRUCTURE VARIATIONS IN $YBa_2Cu_3O_{7-x}$ + $BaSnO_3$ FILMS WITH DIFFERENT CONCENTRATIONS OF $BaSnO_3$ (POSTPRINT)

5a. CONTRACT NUMBER
In-house

5b. GRANT NUMBER

5c. PROGRAM ELEMENT NUMBER
62203F

6. AUTHOR(S)

C.V. Varanasi, J. Burke, and L. Brunke (University of Dayton Research Institute)
H. Wang and J.H. Lee (Texas A&M University)
P.N. Barnes (AFRL/RZPG)

5d. PROJECT NUMBER
3145

5e. TASK NUMBER
32

5f. WORK UNIT NUMBER
314532ZE

7. PERFORMING ORGANIZATION NAME(S) AND ADDRESS(ES)

University of Dayton Research Institute
Dayton, OH 45469

Texas A&M University
College Station, TX 77843-3128

Mechanical Energy Conversion Branch (AFRL/RZPG)
Energy/Power/Thermal Division
Air Force Research Laboratory, Propulsion Directorate
Wright-Patterson Air Force Base, OH 45433-7251
Air Force Materiel Command, United States Air Force

8. PERFORMING ORGANIZATION REPORT NUMBER
AFRL-RZ-WP-TP-2012-0147

9. SPONSORING/MONITORING AGENCY NAME(S) AND ADDRESS(ES)

Air Force Research Laboratory
Propulsion Directorate
Wright-Patterson Air Force Base, OH 45433-7251
Air Force Materiel Command
United States Air Force

10. SPONSORING/MONITORING AGENCY ACRONYM(S)
AFRL/RZPG

11. SPONSORING/MONITORING AGENCY REPORT NUMBER(S)
AFRL-RZ-WP-TP-2012-0147

12. DISTRIBUTION/AVAILABILITY STATEMENT
Approved for public release; distribution unlimited.

13. SUPPLEMENTARY NOTES

14. ABSTRACT

Previous work on $YBa_2Cu_3O_{7-x}$ (YBCO) + $BaSnO_3$ (BSO) films with a single composition showed significant critical current density (J_c) improvements at higher fields but lowered J_c in low fields. A detailed study on BSO concentrations provided here demonstrates that significant J_c enhancement can occur even up to 20 mol% BSO inclusion, where typical particulate inclusions in these concentrations degrade the YBCO performance. YBCO + BSO films were processed on (100) $LaAlO_3$ substrates using premixed targets of $YBa_2Cu_3O_{7-x}$ (YBCO) with additions of 2, 4, 10, and 20 mol% BSO. The critical transition temperature T_c of the films remained high (>87 K), even with large amounts (20 mol%) of BSO. YBCO + BSO films showed a gradual increase in J_c at high fields as the amount of BSO was increased. More than an order of magnitude increase in J_c was measured in YBCO + BSO samples as compared to regular YBCO at 4 T. YBCO + 10 mol% BSO films showed overall improvement at all the field ranges while YBCO + 20 mol% BSO was better only at high fields. Transmission electron microscopy revealed the presence of ~7–8-nm-diameter BSO nanocolumns, the density of which increased with increasing BSO content correlating well with the observed improvements in J_c.

15. SUBJECT TERMS
films, processed, critical, magnitude, transmission, substrates, microscopy, composition, electron

16. SECURITY CLASSIFICATION OF:

a. REPORT	b. ABSTRACT	c. THIS PAGE	17. LIMITATION OF ABSTRACT:	18. NUMBER OF PAGES	19a. NAME OF RESPONSIBLE PERSON (Monitor)
Unclassified	Unclassified	Unclassified	SAR	14	Timothy J. Haugan

19b. TELEPHONE NUMBER *(Include Area Code)*
N/A

Standard Form 298 (Rev. 8-98)
Prescribed by ANSI Std. Z39-18

Critical current density and microstructure variations in YBa$_2$Cu$_3$O$_{7-x}$ + BaSnO$_3$ films with different concentrations of BaSnO$_3$

C.V. Varanasi,[a] J. Burke, and L. Brunke
University of Dayton Research Institute, Dayton, Ohio 45469-0170; and Air Force Research Laboratories, Wright Patterson Air Force Base, Ohio 45433

H. Wang and J.H. Lee
Texas A&M, College Station, Texas 77843-3128

P.N. Barnes
Air Force Research Laboratories, Wright Patterson Air Force Base, Ohio 45433

Previous work on YBa$_2$Cu$_3$O$_{7-x}$ (YBCO) + BaSnO$_3$ (BSO) films with a single composition showed significant critical current density (J_c) improvements at higher fields but lowered J_c in low fields. A detailed study on BSO concentrations provided here demonstrates that significant J_c enhancement can occur even up to 20 mol% BSO inclusion, where typical particulate inclusions in these concentrations degrade the YBCO performance. YBCO + BSO films were processed on (100) LaAlO$_3$ substrates using premixed targets of YBa$_2$Cu$_3$O$_{7-x}$ (YBCO) with additions of 2, 4, 10, and 20 mol% BSO. The critical transition temperature T_c of the films remained high (>87 K), even with large amounts (20 mol%) of BSO. YBCO + BSO films showed a gradual increase in J_c at high fields as the amount of BSO was increased. More than an order of magnitude increase in J_c was measured in YBCO + BSO samples as compared to regular YBCO at 4 T. YBCO + 10 mol% BSO films showed overall improvement at all the field ranges while YBCO + 20 mol% BSO was better only at high fields. Transmission electron microscopy revealed the presence of ~7–8-nm-diameter BSO nanocolumns, the density of which increased with increasing BSO content correlating well with the observed improvements in J_c.

I. INTRODUCTION

It is important to provide flux pinning enhancement in YBa$_2$Cu$_3$O$_{7-x}$ (YBCO)-coated conductors to achieve high critical current densities (J_c) in applied magnetic fields. Such high-J_c conductors are necessary for electrical power applications such as generators and motors, etc., where high magnetic fields are experienced.[1,2] Nanoparticle incorporation[3–6] and rare-earth ion doping[7–9] provide flux pinning centers and are very effective at improving the J_c of YBCO films. In the literature, different groups have shown that nanoparticles can be introduced by different approaches such as multilayers,[3] premixed targets,[4] or sectored targets,[6,10] etc., employing pulsed laser ablation. Different materials such as Y$_2$BaCuO$_5$, BaZrO$_3$, BaSnO$_3$ (BSO), Ir, yttrium-stabilized zirconia, and Y$_2$O$_3$[3–6,11–14] have been investigated for their effectiveness as flux pinning centers. Pulsed laser deposition (PLD) offers a rapid investigation route to determine the compatibility between YBCO and the nanoparticle materials. It is helpful to develop an understanding of the structure–property relationships before adopting nanoparticle additions to other industrial YBCO deposition techniques such as metalorganic deposition (MOD) and metalorganic chemical vapor deposition (MOCVD).

We have recently shown that YBCO + BSO films processed by a dual phase sectored-target approach using a BSO wedge on a YBCO target tend to form BSO nanocolumns that extend through the thickness of the YBCO films.[15] More than an order of magnitude improvement of J_c in these films at high fields was observed as compared to regular YBCO,[10] but they showed a lowered J_c in low fields. Mele et al. recently confirmed the benefits of BSO additions to YBCO,[16] as well. In addition, we have also demonstrated that the curves in flux pinning force (F_p) versus magnetic field plots of these films show the presence of dual peaks with net

maxima (F_{pmax}) shifted to higher fields as compared to regular YBCO[17] or with other additives. However, it was not clear if the improvements and dual peaks in F_p plots observed in the previous study were due primarily to BSO content alone or in part to the particular method of incorporating the material into the YBCO matrix. Also, neither our study[10,17] nor the Mele et al. study[16] considered the effects of varying BSO content and whether some optimal content could be identified for a given magnetic field range. To address these issues, a separate systematic study was undertaken where YBCO + BSO films with increasing concentrations of BSO were made to study the composition–structure–property relationships.

II. EXPERIMENTAL

Commercially available $YBa_2Cu_3O_{7-x}$ powders (Nexans, Hurth, Germany) and $BaSnO_3$ powders (Cerac, Milwaukee, WI) were used to make the targets to deposit YBCO + BSO films with different compositions. The starting powders of $BaSnO_3$ were −325 mesh size. No nanomaterials of BSO were used to make these targets. Different amounts of YBCO and BSO powders were weighed and mixed to make the final targets with 2, 4, 10, and 20 mol% BSO in YBCO. The powders were well mixed with a mortar and pestle to obtain homogeneous mixtures. Disks with the dimensions of 1-in. diameter and 0.25-in. thickness were pressed using a hydraulic press. These disks were sintered at 920 °C for 170 h in air to obtain a final density >90% theoretical density.

Pulsed laser deposition was done in a Neocera (Beltsville, MD) chamber using a Lambda Physik (Santa Clara, CA) excimer (KrF) laser (λ = 248 nm). All the films were grown under identical conditions of 300 mTorr oxygen pressure, 2 J/cm² energy density, 4 Hz rep rate, a substrate-to-heater distance of 6 cm, and a deposition temperature of 780 °C. All the films were oxygen annealed at 500 °C for 30 min in 600 mTorr of oxygen pressure inside the chamber. Films up to a thickness of approximately 300 nm were deposited on (100) $LaAlO_3$ substrates. The film thickness and deposition conditions of all the different film compositions were similar so that the microstructure and properties of the films could be correlated with the BSO content alone, while effects due to other factors were minimized.

An x-ray diffractometer was used to obtain θ-2θ scans on the films to verify the film orientation and composition of the YBCO + BSO films. The critical transition temperature (T_c) was measured by an alternating current (ac) susceptibility method, and the critical current density (J_c) as a function of applied magnetic fields was measured using a vibrating sample magnetometer (VSM; Quantum Design PPMS, San Diego, CA). The VSM data were used to determine the J_c at both 77 and 65 K up to
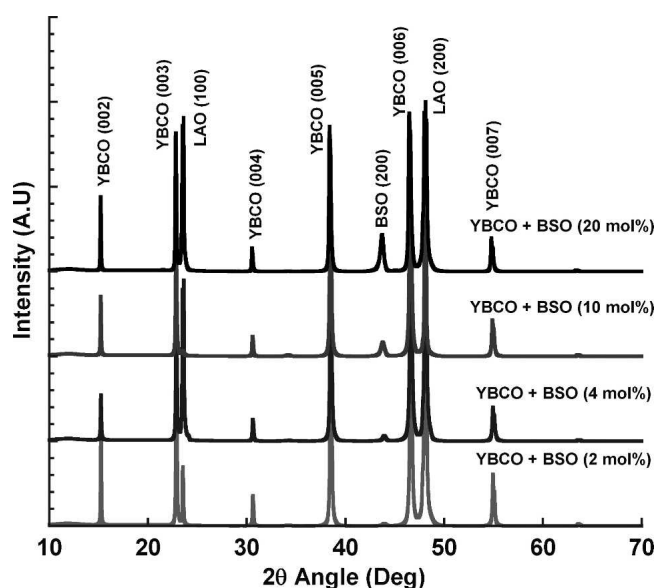

FIG. 1. X-ray θ-2θ scan patterns scans of various YBCO + BSO films.

9 T, employing the Bean model. A KLA Tencor profilometer (Milpitas, CA) was used to determine the film thickness, and these values were then used in the calculations to obtain the magnetization J_c. The microstructures of the films were observed using a SIRION scanning electron microscope (SEM; FEI, Hillsboro, OR). Cross-sectional and plan-view transmission electron microscopy (TEM) studies on all samples were performed using a Philips CM200 analytical electron microscope (FEI) with a point-to-point resolution of 0.21 nm. All the TEM samples were prepared through a conventional TEM sample preparation routine including cutting, gluing, grinding, polishing, and precision ion polishing.
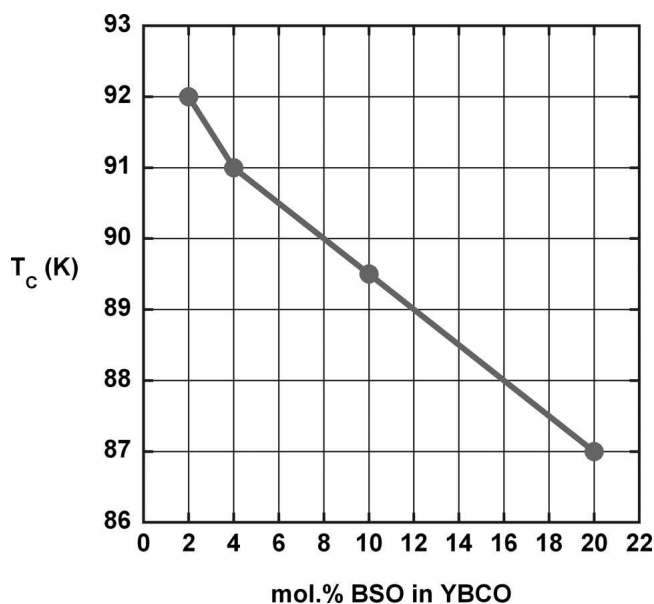

FIG. 2. T_c variation in YBCO + BSO films with varying BSO content.

III. RESULTS AND DISCUSSION

Figure 1 shows the θ-2θ scan patterns (normalized with the highest peak intensity of each sample) of different films processed in this study. It can be seen that all the films are c-axis-oriented, showing only YBCO (00l) peaks. Peaks corresponding to only the BSO (200) reflections were noted at ~44°, indicating that BSO is also well oriented in the films. In addition, the intensity of the BSO (200) peaks increased as the mol% of BSO in the films was increased, indicating that the (200) orientation was maintained as the BSO content increased. No addi-

tional peaks corresponding to any other phases were observed, indicating that the BSO is probably inert in YBCO at these processing conditions.

The T_c values of different YBCO + BSO films are plotted in Fig. 2 as a function of BSO content. It can be seen that a high T_c of ~92 K was found for the YBCO + 2 mol% BSO films, which is similar to plain YBCO films; however, as the content of BSO was increased, a gradual decrease in T_c was observed. Even though the films had 20 mol% BSO content, they still showed a reasonably high T_c of 87 K. These results are in stark contrast to BaZrO$_3$ (BZO) additions to YBCO films where a significant drop in T_c was observed[18,19] when the BZO content was increased. It is possible that some Sn diffusion into YBCO films can occur during PLD. It has been shown previously that a drop in T_c can be expected if Sn is substituted for Cu sites in bulk YBCO.[20] The observed minor drop in T_c may be attributed to these Sn substitutions or to the total strain in the YBCO lattice due to a lattice mismatch between BSO and YBCO that may increase as the BSO content is increased; however, it appears that these effects are limited and do not reduce the T_c significantly below 87 K, even up to 20 mol% of BSO additions. It should be noted that even though the T_c in YBCO + 20 mol% BSO films is lowered to 87 K, it is still much higher than the operating temperature of many applications (77 or 65 K), and the effect of T_c reduction on J_c seems to be minimal at these temperatures, as will be discussed later.

Figure 3 shows the magnetization J_c of YBCO + BSO films with different amounts of BSO at 77 and 65 K as a function of magnetic field in the $H//c$ orientation. It can be seen that the YBCO + BSO films show more than an order of magnitude improvement over regular YBCO films at fields >4 T and nearly 2 orders of magnitude improvement at even higher fields >6 T. Even at lower fields (<2 T), the improvement is significant in low doping levels of BSO (e.g., YBCO + 10 mol% BSO) samples. At low fields, the amount of BSO in the films does not participate in the flux pinning enhancement (due to a lower density of fluxons) and detracts from the overall superconducting volume of the film. For the YBCO + 20 mol% BSO films, the observed decrease in J_c below 1 T is due at least in part to this contribution of non-superconducting volume of BSO in the films. However, due to a large number of fluxons, the interaction between the BSO nanocolumns (to be discussed later) and fluxons is more fully utilized and results in enhanced pinning as evidenced by the significantly increased J_c at high fields. Transport current J_c measurements taken on one of the samples (YBCO + 20 mol% BSO) correlated well with the magnetization J_c data presented here, especially at high fields. However, the magnetization J_c in low fields (<4 T) was found to be lower than the transport J_c for the reasons explained above.
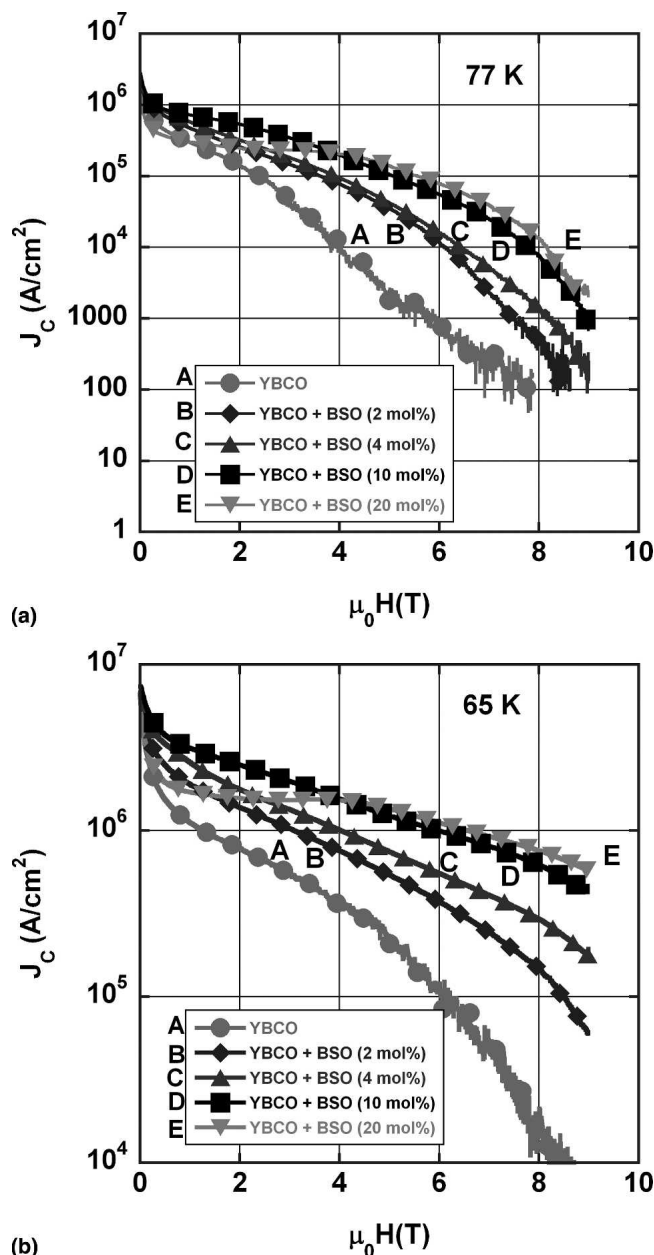

FIG. 3. Magnetization J_c of YBCO + BSO films as a function of applied magnetic field with varying amounts of BSO content as compared to regular YBCO (a) at 77 K and (b) at 65 K.
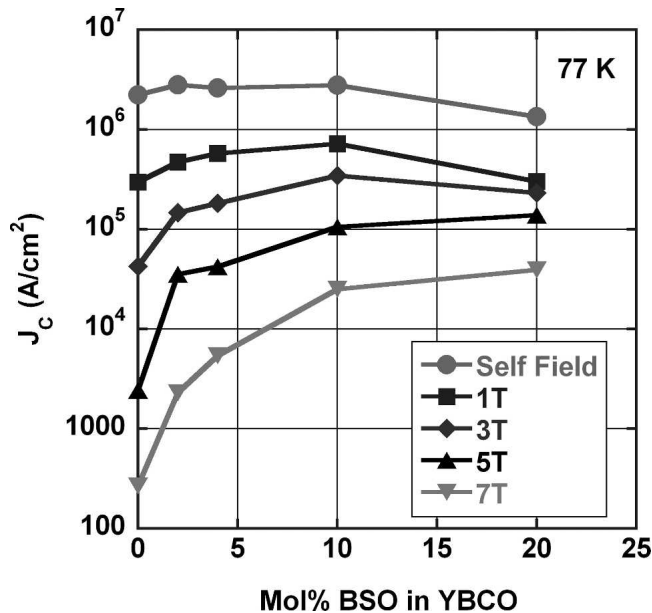
3

FIG. 4. Magnetization J_c of YBCO + BSO films as a function of the BSO content at various magnetic fields at 77 K.

Figure 4 shows the 65 K J_c data plotted for YBCO samples with different BSO concentrations at different magnetic fields (1–7 T) to more clearly depict the effects of BSO content on the J_c in these films. It can be clearly seen that the effect of BSO content on J_c seems to depend upon the field of measurement. For example, self-field J_c or J_c at low fields (<3 T) decreases slightly by increasing the BSO content from 2 to 20 mol%. However, with the same change in composition, the J_c was found to increase significantly at higher fields such as 5 or 7 T. It should be noted that all the films show improvement over regular YBCO data (shown as a sample of YBCO + BSO, 0 mol%, Fig. 4) at high fields. The optimum level seems to be 10 mol% BSO for the applications below 3 T. For higher field applications, a higher level may be suitable, although the improvements in J_c seem to indicate that it could approach a plateau above 20 mol%. However, it should be noted that higher amounts could further reduce the low-field J_c data, even though slightly higher J_c at high fields may be obtained. In the YBCO + BSO films with higher BSO amounts (~30 mol%) prepared with a 30° BSO wedge, such degradation in low fields was observed, even though high field performance was enhanced.[10] Thus, it appears that the optimum BSO content in YBCO depends upon the intended application. YBCO + 10 mol% BSO seems to have optimum performance in the magnetic field range of 0–4 T and YBCO + 20 mol% seems to be optimum in 4–9 T range.

The YBCO + 10 mol% BSO films had a low α value of 0.36, and YBCO + 20 mol% BSO films had an α value
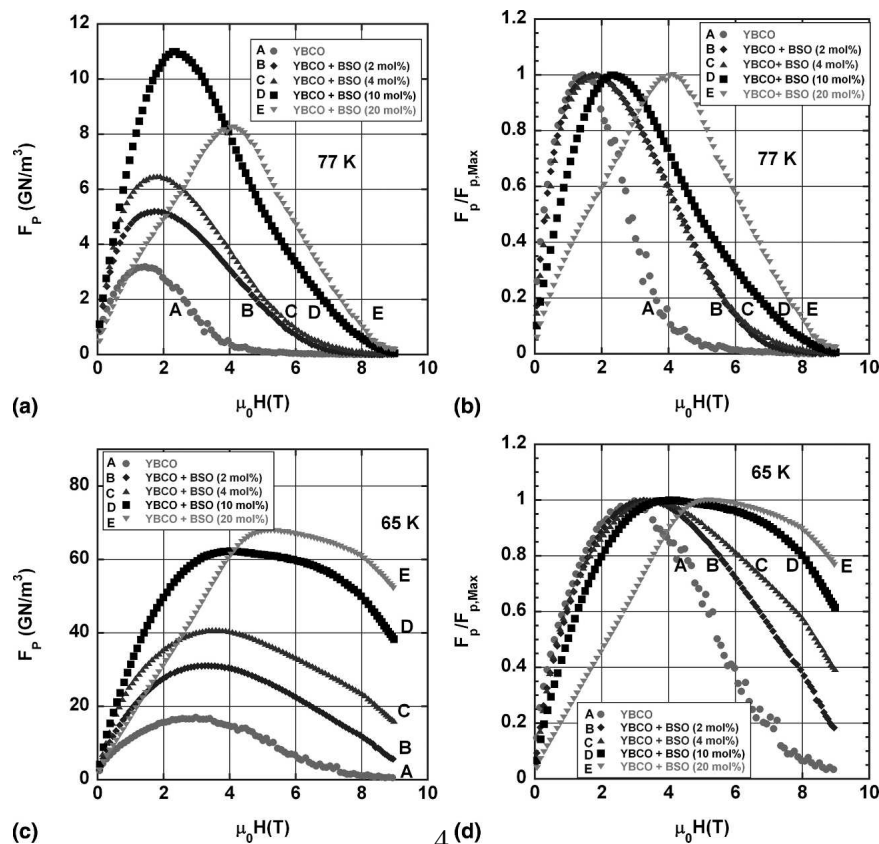

FIG. 5. Flux pining force (F_p) of different YBCO + BSO films (a) F_p at 77 K, (b) F_p/F_{pmax} at 77 K, (c) F_p at 65 K, and (d) F_p/F_{pmax} at 65 K.

Approved for public release; distribution unlimited

of 0.38 at 77 K as compared to a regular YBCO film that usually has an α value of 0.5.[21] However, YBCO + 2 mol% BSO had an α value close to 0.5. A lower α value indicates a less rapid decrease in J_c with an increase in magnetic field. Similar low α values were also noted in other YBCO films with nanocolumns, and the present trend of lowered α with increased nanocolumns is consistent with improved pinning.[4,21,22]

Figure 5 shows the pinning force F_p versus B plots at 77 and 65 K. Of particular interest is that the F_p peak maximum (F_{pmax}) continues to increase in value as the BSO content is increased at 65 K but only up to 10 mol% in the case of 77 K. In Figs. 5(b) and 5(d), the normalized $F_p/F_{p\ max}$ versus magnetic field is plotted to show the shifts in the peak position. It can be seen that the peak position moves to higher fields as the BSO content is increased at both 65 and 77 K. The F_p peak in YBCO + 20 mol% BSO occurs at as high as 4 T at 77 K. In addition, the overlapping dual peak structure become discernible in the F_p plots of YBCO + 20 mol% BSO content at 77 K, similar to the plots seen in YBCO + BSO films containing higher BSO content.[17] The presence of the dual peak structure (where the composite overlapping dual peak structure has a main peak with a shoulder) in the F_p plots of YBCO + BSO with higher BSO content as shown in this work is reproducible from previous work and apparently is process independent, depending largely upon the amount of BSO content in the film. The presence of the dual peak structure and peak shifts in the F_p plots signify the potential fundamental changes in the pinning mechanisms that may be operative in the samples as the BSO content is increased, as previously discussed.[17]

In SEM characterization of the microstructures, the presence of 0.4–0.5-μm particles, as well as thoroughly dispersed nanoparticles, was observed in all the samples. Figure 6 shows SEM images of a YBCO + BSO (4 mol%) sample as an example. As the BSO content was increased, the number density of these nanoparticles as seen in the plan-view SEM images increased. These nanoparticles could be BSO nanocolumns as seen by cross-sectional TEM images (discussed later) projected on a two-dimensional plane. The presence of the larger particles does occur at times in PLD films and is generally attributed to particle/grain transfer that happens from the target to the films. Typically, these large particles are not expected to participate in the flux pinning enhancement due to their large size as compared to coherence length of YBCO.

Figure 7 shows the TEM plan-view and cross-sectional images of different composition samples (YBCO with 2 and 20 mol% BSO). As the BSO content was increased, the density of the nanoparticles, as seen in plan view, also increased. In the cross-sectional TEM, well-separated uniform-diameter nanocolumns extended throughout the thickness of the films. It is possible that
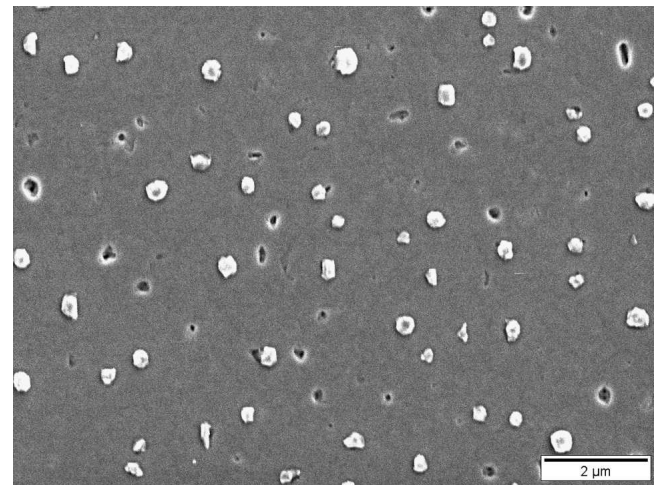
(a)
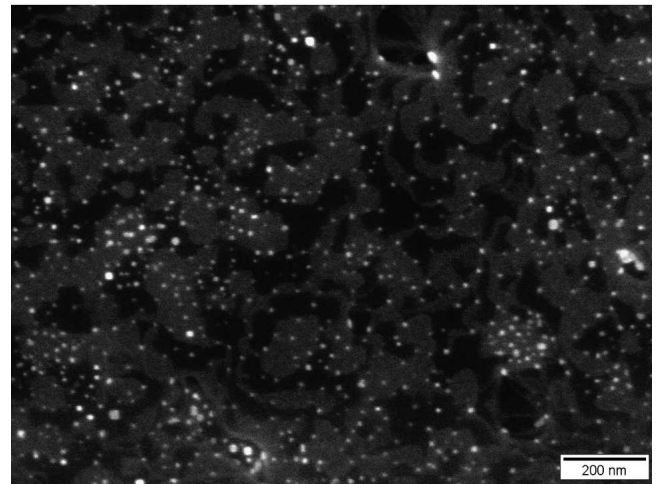
(b)

FIG. 6. Scanning electron micrograph showing the BSO nanoparticles in a YBCO + 4 mol% BSO sample: (a) low magnification micrograph showing large particles and (b) high magnification micrograph showing nanoparticles in plan view.

the nanocolumns seen in the cross-sectional view account for most of the nanoparticles observed in the plan view TEM or SEM. Due to the lattice mismatch between BSO and YBCO (~7.7%), Moiré patterns are observed in the microstructure. Selected-area diffraction patterns taken from these nanocolumns confirmed that they are indeed BSO. The number density of these nanocolumns increased to as high as 1.5×10^{11}/cm^2 in YBCO + 20 mol% BSO samples while the average diameter of the nanocolumns remained relatively constant at ~7–8 nm. The average spacing between them decreased from 50 to 20 nm as the BSO content was increased from 2 to 20 mol%. It should be noted that although no nanoparticle BSO was used in the target manufacture, the BSO nanocolumns were formed in the films. It is believed that the strain in the matrix of the YBCO favors such nucleation and growth of BSO nanocolumns.
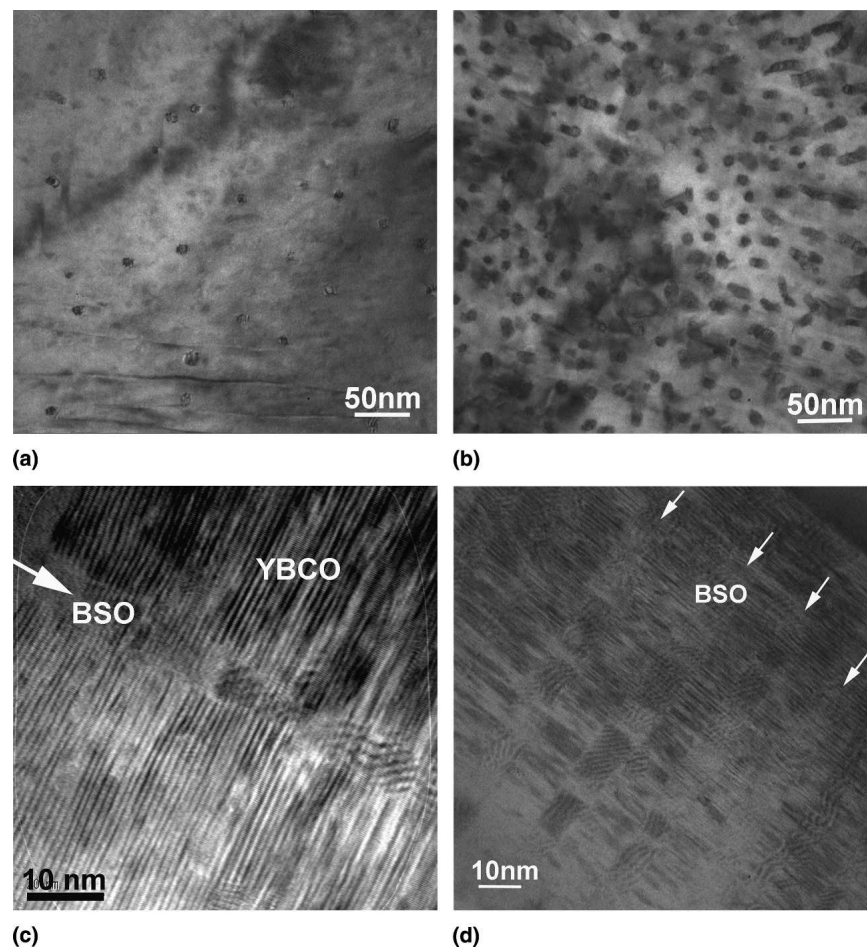
FIG. 7. TEM images showing (a) YBCO + 2 mol% BSO plan view, (b) YBCO + 20 mol% BSO plan view, (c) YBCO + 2 mol% BSO cross-section, and (d) YBCO + 2 mol% BSO cross-section view.

A one-to-one correlation with the microstructure consisting of the BSO nanocolumns and the J_c properties is clearly seen in the present study. An increase in the number density of the nanocolumns seems to help to increase the high-field J_c. Local lattice mismatching and the associated strain fields continue to help form the nanocolumns to a very high density as supported by theoretical predictions.[23] What is apparent is that the BSO nanocolumns of similar diameter continue to form even when the content is increased to 20 mol%, and no coalescence between the columns is observed. Such a microstructure is found to be beneficial for J_c property enhancement if the T_c can be maintained reasonably high.

IV. CONCLUSIONS

The YBCO + BSO films with gradual increase in the amount of BSO showed a corresponding increase in J_c and the number density of nanocolumns (~7–8 nm diameter). With BSO, the T_c remained higher, unlike other materials, thus allowing the incorporation of a high den-

sity of nanocolumns. Compared to regular YBCO, nearly two orders of magnitude improvement in J_c was observed in YBCO + 20 mol% BSO films showing a value of ~10^5 A/cm^2 at 6 T and ~10^4 A/cm^2 at 8 T at 77 K. In lower fields (0–4T), YBCO + 10 mol% BSO showed improved J_c over all the compositions. The incorporation of such a large percentage of non-superconducting material into the YBCO matrix has previously degraded its performance as opposed to the BSO work presented here. It is possible to tailor the J_c properties of YBCO with different amounts of BSO for different applications.

REFERENCES

1. D. Larbalestier, A. Gurevich, D.M. Feldman, and A. Polyanski: High T_c superconducting materials for electric power applications. *Nature* **414,** 368 (2001).

2. P.N. Barnes, M.D. Sumption, and G.L. Rhoads: Review of high power density superconducting generators: Present state and prospects for incorporating YBCO windings. *Cryogenics* **45,** 670 (2005).

3. T.J. Haugan, P.N. Barnes, R. Wheeler, F. Meisenkothen, and M. Sumption: Addition of nanoparticle dispersions to enhance flux pinning of the $YBa_2Cu_3O_{7-x}$ superconductor. *Nature* **430,** 867 (2004).

4. J.L. MacManus-Driscoll, S.R. Foltyn, Q.X. Jia, H. Wang, A. Serquis, L. Civale, B. Maiorov, M.E. Hawley, M.P. Maley, and D.E. Peterson: Strongly enhanced current densities in superconducting coated conductors of $YBa_2Cu_3O_{7-x}$ +$BaZrO_3$. *Nat. Mater.* **3,** 439 (2004).

5. S. Kang, A. Goyal, J. Li, A.A. Gapud, P.M. Martin, L. Heatherly, J.R. Thomson, D.K. Christen, F.A. List, M. Paranthaman, and D.F. Lee: High-performance high-T_c superconducting wires. *Science* **311,** 1911 (2006).

6. C. Varanasi, P.N. Barnes, J. Burke, J. Carpenter, and T.J. Haugan: Controlled introduction of flux pinning centers in $YBa_2Cu_3O_{7-x}$ films during pulsed laser deposition. *Appl. Phys. Lett.* **87,** 262510 (2005).

7. C. Varanasi, R. Biggers, I. Maartense, D. Dempsey, T.L. Peterson, J. Solomon, J. McDaniel, G. Kozlowski, R. Nekkanti, and C.E. Oberly: Pulsed laser deposition of Nd-doped $Yba_2Cu_3O_{7-x}$ films for coated conductor applications, in *Advances in Laser Ablation of Materials*, edited by R.K. Singh, D.H. Lowndes, D.B. Chrisey, E. Fogarassy, and J. Narayan (Mater. Res. Soc. Symp. Proc. **526,** Warrendale, PA, 1998), p. 263.

8. X. Song, Z. Chen, S. Kim, D. Feldman, D. Larbalestier, J. Reeves, Y. Xie, and V. Selvamanickam: Evidence for strong flux pinning by small, dense nanoprecipitates in a Sm-doped $YBa_2Cu_3O_{7-\delta}$ coated conductor. *Appl. Phys. Lett.* **88,** 212 (2006).

9. H. Zhou, B. Mairov, H. Wang, J.L. MacManus-Driscoll, T.G. Holesinger, L. Civale, Q.X. Jia, and S.R. Foltyn: Improved microstructure and enhanced low-field J_c in $(Y_{0.67}Eu_{0.33})Ba_2Cu_3O_{7-\delta}$ films. *Supercond. Sci. Technol.* **21,** 025001 (2008).

10. C.V. Varanasi, P.N. Barnes, J. Burke, L. Brunke, I. Maartense, T.J. Haugan, E.A. Stinzianni, K.A. Dunn, and P. Haldar: Flux pinning enhancement in $YBa_2Cu_3O_{7-x}$ films with $BaSnO_3$ nanoparticles. *Supercond. Sci. Technol.* **19,** L37 (2006).

11. J. Hänisch, C. Cai, R. Hühne, L. Schultz, and B. Holzapfel: Formation of nanosized $BaIrO_3$ precipitates and their contribution to flux pinning in Ir-doped $YBa_2Cu_3O_{7-\delta}$ quasi-multilayers. *Appl. Phys. Lett.* **86,** 122508 (2005).

12. P. Mele, K. Matsumato, T. Horide, A. Ichinose, M. Mukaida, Y. Yoshida, and S. Horii: Enhanced high-field performance in PLD films fabricated by ablation of YSZ-added $YBa_2Cu_3O_{7-x}$ target. *Supercond. Sci. Technol.* **20,** 244 (2007).

13. T.A. Campbell, T.J. Haugan, I. Maartense, J. Murphy, L. Brunke, and P. Barnes: Flux pinning effects of Y_2O_3 nanoparticulate dispersions in multilayered YBCO thin films. *Physica C* **423,** 1 (2005).

14. A. Goyal, S. Kang, K.J. Leonard, P.M. Martin, A.A. Gapud, M. Varela, M. Paranthaman, A.O. Ijaduola, E.D. Specht, J.R. Thomson, D.K. Christen, S.J. Pennycook, and F.A. List: Irradiation-free, columnar defects comprised of self-assembled nanodots and nanorods resulting in strongly enhanced flux-pinning in $YBa_2Cu_3O_{7-\delta}$ films. *Supercond. Sci. Technol.* **18,** 1533 (2005).

15. C.V. Varanasi, J. Burke, L. Brunke, H. Wang, M. Sumption, and P.N. Barnes: Enhancement and angular dependence of transport critical current density in pulsed laser deposited $YBa_2Cu_3O_{7-x}$ + $BaSnO_3$ films in applied magnetic fields. *J. Appl. Phys.* **102,** 063909 (2007).

16. P. Mele, K. Matsumoto, T. Horide, A. Ichinose, M. Mukaida, Y. Yoshida, S. Horii, and R. Kita: Ultra-high flux pinning properties of $BaMO_3$-doped $YBa_2Cu_3O_{7-x}$ thin films (M = Zr, Sn). *Supercond. Sci. Technol.* **21,** 032002 (2008).

17. C.V. Varanasi, P.N. Barnes, and J. Burke: Enhanced flux pinning force and uniquely shaped flux pinning force plots observed in $YBa_2Cu_3O_{7-x}$ films $BaSnO_3$ nanoparticles. *Supercond. Sci. Technol.* **20,** 1071 (2007).

18. S. Kang, A. Goyal, J. Li, P. Martin, A. Ijaduola, J.R. Thomson, and M. Paranthaman: Flux-pinning characteristics as a function of density of columnar defects comprised of self-assembled nanodots and nonorods in epitaxial $YBa_2Cu_3O_{7-x}$ films for coated conductor applications. *Physica C* **457,** 41 (2007).

19. M. Perula, P. Paturi, Yu.P. Stepanov, H. Huhtinen, Y.Y. Tse, A.C. Bodi, J. Raittila, and R. Laiho: Optimization of the $BaZrO_3$ concentration in YBCO films prepared by pulsed laser deposition. *Supercond. Sci. Technol.* **19,** 767 (2006).

20. J. Feng, K.K. Yeung, K.W. Wong, E.C.L. Fu, and C.C. Lam: Powder XRD investigation of crystal structure modification effects on superconductivity in the Sn–doped YBa_2Cu_3 Sn_xO_{7-d} systems. *Supercond. Sci. Technol.* **13,** 215 (2000).

21. A.A. Gapud, D. Kumar, S.K. Viswanathan, C. Cantoni, M. Varela, J. Abiade, S.J. Pennycook, and D.K. Christen: Enhancement of flux pinning in $YBa_2Cu_3O_{7-\delta}$ thin films embedded with epitaxially grown Y_2O_3 nanostructures using a multi-layering process. *Supercond. Sci. Technol.* **18,** 1502 (2005).

22. M.D. Sumption, T.J. Haugan, P.N. Barnes, T.A. Campbell, N.A. Pierce, and C. Varanasi: Magnetization creep and decay in $YBa_2Cu_3O_{7-x}$ thin films with artificial nanostructure pinning. *Phys. Rev. B* **77,** 094506 (2008).

23. J.P. Rodriguez, P.N. Barnes, and C.V. Varanasi: In-field critical current of type-II superconductors caused by strain from nanoscale columnar inclusions. *Phys. Rev. B* **78,** 052505 (2008).

7